



P11

ONE EXAMPLE OF USEFUL DISORDER : STRUCTURE OF PR(III) COMPLEX OF 1,4,7,10-TETRAAZACYCLODODECANE-10-METHYL-1,4,7-TRIS(METHYLENEPHENYL PHOSPHINIC) ACID

Jana Klimentová, Pavel Vojtíšek*

Department of Inorganic Chemistry, Faculty of Science, Charles University, Hlavova 2030, Prague 2, 128 43, Czech Republic, *pavojt@natur.cuni.cz

Coordination chemistry of lanthanide ions and yttrium with N,O-macrocyclic ligands is widely investigated because of the importance of their medicinal and biochemical use, such as Gd^{3+} complexes as contrast agents (CA) in magnetic resonance imaging (MRI) [1,2], ^{90}Y complexes in radioimmunotherapy [2] and luminescent Eu^{3+} and Tb^{3+} compounds as probes [2,3]. Previously, we published [4] an interesting set of structures of complexes of 1,4,7,10-tetraazacyclododecane-10-methyl-1,4,7-tris(methylenephosphinic) acid (H_3L , see Figure 1). This acid forms neutral dimeric complexes $[LnL(H_2O)_n]_2 \cdot x H_2O \cdot y MeOH$ with Ln^{3+} ions, where $n = 0$ or 1, $x = 5-7$ and $y = 0-2$, for different Ln^{3+} [4]. All compounds are isostructural and crystallise in space group $P2_1/c$ (no. 14) with similar values of lattice parameters and similar position of the lanthanide ion in the unit cell.

However, the compound $[PrL(H_2O)_n]_2 \cdot x H_2O$ does not belong to the previously published isostructural set. The structure investigation of $[PrL(H_2O)_n]_2 \cdot x H_2O$ has resulted in an interesting conclusion [5]. The successful modelling of disorders in this case gave us a picture of "frozen solution" with samples of isomeric species present. Three chemically and four crystallographically different complexes were identified and structurally characterised: $[Pr\{L(R,S)\}]_2$ with coordination number (CN) 8, $[Pr\{L(R,R)\}(H_2O)]_2$ with CN 9 and two species $[Pr\{L(R,S)\}(H_2O)]_2$ also with CN 9, but with a little different geometrical parameters (the symbols L(R,R) and L(R,S) mean the different chirality on phosphorus atom of the ligand labelled P2 in the resulting complex, respectively). Therefore, the title compound should be written as

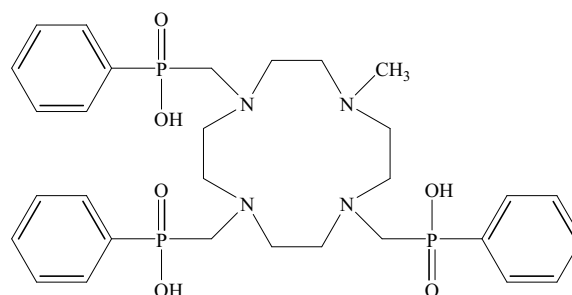


Fig 1. The formula of H_3L .

$0.67 [Pr\{L(R,R)\}(H_2O)]_2 \cdot 0.33 [Pr\{L(R,S)\}(H_2O)]_2 \cdot 0.67 [Pr\{L(R,S)\}]_2 \cdot 0.33 [Pr\{L(R,S)\}(H_2O)]_2 \cdot 27.5 H_2O$.

In our opinion, it illustrates that disorder can represent not only a nuisance in structure solving and refinement; it may bring useful chemical information as well.

1. The Chemistry of Contrast Agents in Medical Magnetic Resonance Imaging, eds. A. E. Merbach, É. Tóth, Wiley, Chichester, U. K. (2001); Topics in Current Chemistry, Springer, Frankfurt am Main, Germany **221** (2002).
2. D. Parker, in Comprehensive Supramolecular Chemistry, ed. J.-M. Lehn, Pergamon, Oxford, **10** (1996) 487.
3. S. Faulkner, J. L. Matthews, in Comprehensive Coordination Chemistry II, eds. J. A. McCleverty, T. J. Meyer, Elsevier, Amsterdam **9** (2004) 913 and refs. therein.
4. J. Rohovec, P. Vojtíšek, I. Lukeš, P. Hermann, J. Ludvík, *J. Chem. Soc., Dalton Trans.* (2000) 141.
5. J. Klimentová, P. Vojtíšek, *J. Mol. Struct.*, accepted for publication.

P12

STRUCTURE OF MONTMORILLONITE INTERCALATED WITH METHYLENE BLUE. MOLECULAR SIMULATIONS AND EXPERIMENT

M. Pospíšil¹, R. Macháň¹, P. Malý¹, Z. Klika², P. Čapková^{1,2}, P. Horáková², M. Valášková²

¹Faculty of Mathematics and Physics, Charles University Prague, Ke Karlovu 3, 12116, CZ

²VŠB-Technical University Ostrava, 708 33 Ostrava-Poruba, CZ, pospisil@karlov.mff.cuni.cz

Structure analysis using combination of experimental (X-ray powder diffraction, infrared spectroscopy, fluorescence, etc.) and theoretical (molecular simulations) methods is powerful tool for solving disordered structures. In this work the structures of two different types of montmorillonites (MMT) intercalated with methylene blue cations are solved. Crystallochemical formula of Wyoming MMT is $\text{Na}_{0.41}\text{K}_{0.14}\text{Ca}_{0.07}(\text{Al}_{3.01}\text{Mg}_{0.48}\text{Fe}^{3+}_{0.49})[\text{Si}_{7.81}\text{Al}_{0.17}\text{Ti}_{0.02}]\text{O}_{20}(\text{OH})_4$ and Ca-Cheto MMT: $\text{Na}_{0.10}\text{K}_{0.04}\text{Ca}_{0.50}(\text{Al}_{2.80}\text{Mg}_{1.00}\text{Fe}^{3+}_{0.20})[\text{Si}_{7.86}\text{Al}_{0.14}]\text{O}_{20}(\text{OH})_4$. The fully intercalated samples of Wyoming and Cheto MMT with methylene blue cations were prepared repeated intercalation by methylene blue solutions. The concentration of methylene blue in solutions was determined by photometry method (UV-VIS spectrophotometer – Lambda 25, Perkin Elmer). X-ray powder diffraction (XRPD) measurements were carried out in INEL X-ray powder diffract meter. Fluorescence was excited using a He-Cd laser at 325 nm. Molecular simulations were carried out in *Cerius*² modelling environment [1] to describe the structure characterization obtained from XRPD. Initial model of montmorillonite: space group *C2/m*, the unit cell parameters: $a = 5.208 \text{ \AA}$ and $b = 9.020 \text{ \AA}$ [2]. To create the supercell of reasonable size for calculations, the structural formula determined from chemical analysis was slightly modified. That means for Wyoming MMT the supercell $3a \ 2b \ 1c$ with the layer composition $(\text{Al}_{18}\text{Mg}_3\text{Fe}^{3+}_3)(\text{Si}_{47}\text{Al}_1)\text{O}_{120}(\text{OH})_{24}$ was built with the total negative layer charge (-4) and for Cheto MMT the supercell $3a \ 2b \ 1c$ with the layer composition $(\text{Al}_{17}\text{Mg}_6\text{Fe}^{3+}_1)(\text{Si}_{47}\text{Al}_1)\text{O}_{120}(\text{OH})_{24}$ was built with the total negative layer charge (-7). The potential energy was described with Universal force field [3], charges were calculated by Charge equilibration [4] and minimization was done in *Minimizer* module with fix cell parameters: a, b, c . Quench molecular dynamics simulations in NVT ensemble was done for minimized models. Temperature was $T = 300 \text{ K}$ and kept constant using Berendsen thermostat [5], silicate layers were fixed during dynamic simulation.

The amount of MB intercalated into MMT increase with increasing MB concentration in the intercalation solution. Different amount of MB cations was placed in the interlayer space of MMT to built models for fully and partially exchanged MB-MMT. Optimized structures for the fully exchanged MB-Wyoming MMT (4 MB⁺ cations per supercell) led to the basal spacing 1.77 nm and for partially exchanged MB-Wyoming MMT (2 MB⁺ and 2 Na⁺ cations per supercell) exhibit the basal spacing in the range 1.51 – 1.53 nm. The arrangement of MB guests is monolayer with MB planes slightly tilted and the long axis almost parallel with the silicate layers. Modeling of MB-Cheto MMT led

to the similar results. Models of fully exchanged MB-Cheto MMT (7 MB⁺ cations per supercell) led to the basal spacing 2.03 nm and where MB⁺ cations create bilayer arrangement of MB dimmers with the tilting angles higher than in case of MB-Wyoming MMT. Optimized structure of the partially exchanged MB-Cheto MMT (4 MB⁺ and 3 Na⁺ cations per supercell) exhibits the basal spacing 1.77 nm. Comparison of calculated basal spacing with the experimental values confirmed the conclusion, that the samples of Wyoming and Cheto MMT were saturated but not fully exchanged. According to molecular modelling the basal spacing calculated for the fully exchanged Cheto MMT was 2.03 nm, which means that the samples MB-Cheto MMT with experimentally measured basal spacing 1.71 nm and 1.86 nm were fully not fully exchanged.

Fluorescence measurements for MB-Wyoming MMT show very similar band profile covering a wide wavelength range for all investigated samples. In opposite of this the fluorescence intensity is very low nearly negligible for MB-Cheto. The high layer charge in Cheto MMT requires the high MB⁺ concentration in the interlayer. MB⁺ cations interact with negatively charged silicate layer, with neighbouring guests and also with the rest of exchangeable cations in the interlayer space. Consequently the charge transfer between MB⁺ cations and their environment is enhanced and the fluorescence intensity decreased.

Structure analysis using combination of diffraction data with molecular modelling revealed the differences in the interlayer arrangement of MB⁺ guests in Wyoming and Cheto MMT. Moreover fluorescence measurements showed the strong effect of the silicate layer charge on the spectroscopic behaviour of MB⁺ guests intercalated in MMT. Methylene blue exhibits the strong luminescence in Wyoming MMT and almost no luminescence in Cheto MMT.

1. *Cerius*² documentation, Molecular Simulations Inc. San Diego (June 2000), (CD-ROM).
2. S. I. Tshipursky and V. A. Drits, *Clay Miner.*, **19** (1984) 177.
3. A. K. Rappé, C. J. Casewit, K. S. Colwell, W.A.III. Goddard, W.M. Skiff, *J. Am. Chem. Soc.*, **114** (1992) 10024.
4. A. K. Rappé and W. A. III Goddard, *J. Phys. Chem.*, **95** (1991) 3358.
5. H. J. C. Berendsen, J. P. M. Postma, W. F. van Gunsteren, A. DiNola, J. R. Haak, *J. Chem. Phys.*, **81** (1984) 3684.

This research was supported by VZ MSMT 0021620835, 6198910016 and GA ČR 205/03/D111, 205/05/2548.



P13

APPLICATION OF X-RAY POWDER MICRODIFFRACTION IN NON-DESTRUCTIVE MICROANALYSIS OF COLOUR LAYERS AND MICROTRACES

V. Šímová Grunwaldová¹, M. Kotrlý², P. Bezdička¹, E. Kotulanová¹, D. Hradil¹

¹*Institute of Inorganic Chemistry ASCR, 250 68 Rez, Czech Republic*

²*Institute of Criminalistics Prague, Strojnicka 27, PO box 62/KUP, 170 82 Prague 7, Czech Republic
veronika@iic.cas.cz*

Introduction

Analysis of pigment phases is one of standard operations in many material fields as well as in the forensic science sphere. It is required for expert examination of a whole range of evidence (car paints, abrasion of lacquer systems of tools and instruments, fragments of interior and exterior paints and plaster coats, painting pigments etc. – exhaustive listing could be very lengthy). The existing analytical practice, requiring the sample to be divided for individual instrumental methods, was beginning to prove unsatisfactory because in a number of cases stated above it is necessary to study every single layer separately and the results of stratigraphy studies can contribute to expression or dismissal of the generic match possibility in comparisons. Furthermore, considering the sample inhomogeneity, it was often possible to arrive at misleading information.

Methodology

Therefore, the Institute of Criminalistics Prague in cooperation with the Institute of Inorganic Chemistry of the ASCR and Academy of Fine Arts in Prague verified in practice the methodology of a complex technique that would allow maximum number of determinations from a single sample/fragment, or from its exactly defined areas. The method is based on polished sections and thin microtome sections, on which methods of optical microscopy and fluorescence, SEM/EDS, FTIR, m-XRD etc. are applied. Individual methods are working on the very same spots, or areas of stratigraphic set layers.

The role of powder microdiffraction, which in most cases allows direct exact phases identification, is important in this complex methodology. Measurements were made on an X'PertPro diffractometer made by a Dutch company PANalytical. It is a combination of a common X-ray tube, a capillary, which focuses the X-ray beam into the diameter of 0.1 mm, and a position-sensitive detector. The set enables phase analysis from the area of hundreds of square micrometers in hours.

It was established that successful measurement of raw samples is possible, e.g. artwork fragments, layers applied on mats of various shapes (glass slide, thin wire etc.) or powders. At the same time it is possible to measure samples fixed in the filler and polished in their cross section, or microtome sections from these filled samples. Only such polished section allows measurement of each layer in technological sequence. With raw fragments it is sometimes very difficult to find the measuring area, so that in the area of low angles there is no shading caused by surface unevenness. In the case of polished sections, problematic are

fillers most commonly on the basis of polyester resin, which causes diffraction lines widening and worsens background noise. The same effect applies to generally present organic binders in samples of colour layers in paintings or polychromy. For sample adjustment, a thin silicone non-diffractive mat proved useful. It is made of monocrystalline silicone drawn in the direction (100). The ingot was then cut into slices of 0.3 mm in such a way, that the cut was conducted in the angle of 7 degrees to the plane perpendicular to growth direction (100). Thus, the diffraction phenomenon does not occur in the mat material. These mats can be used universally and apart from XRD analysis, also transmission FTIR and SEM/EDS can be performed from one cut adjustment. With SEM/EDS it is in some cases necessary to lower the operating voltage with ultrathin sections).

Perfectly polished section in clear filler, which does not demonstrate UV luminescence, is optimal for the purposes of optical microscopy, SEM/EDS and colorimetry. Microscopic methods are realized first; therefore the polishing step cannot be left out. However, for the purposes of powder X-ray microdiffraction it is necessary to roughen the polished section surface or cut it – to get rid of the filler traces, which contaminate it during polishing. For IR microspectrometry both the filler and rough surface bring complications – therefore the best surface treatment is microtome cutting or the preparation of a microtome section for transmission measuring.

Measuring geometry of powder X-ray microdiffraction can be changed for samples of various heights. It is necessary to eliminate as much as possible the contribution of the



Fig. 1. Microphotograph of the painting sample section with indicated measuring points.

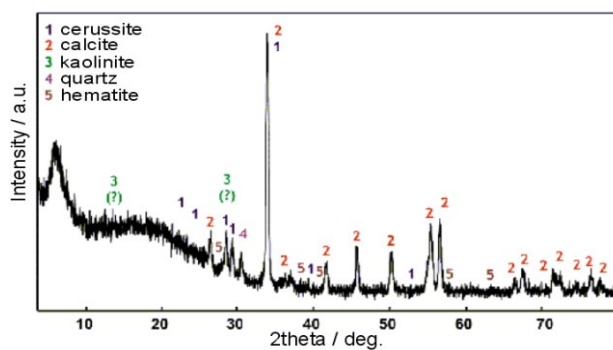


Fig. 2. Powder diffraction pattern of the sample section brown underlayer in point 2.

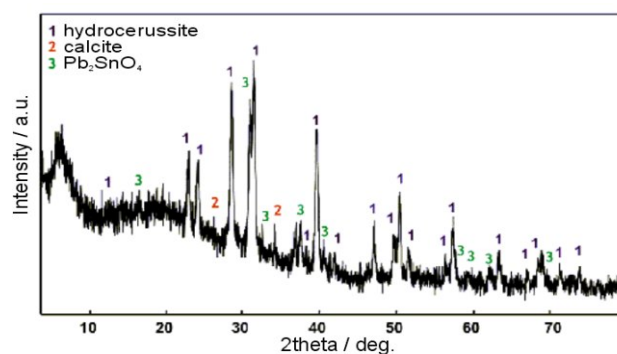


Fig. 3. Powder diffraction pattern of the sample section yellow colour layer in point 3.

filler into the whole analytical signal of polished and microtome sections measurement. Although this contribution does not disable the measurement itself, the interpretation of the consequent diffractogram is influenced in the area of low angles in case of all types of fillers. It is necessary to take into account that the detection limit of phase determination with light elements is ca. 5 mass %.

Fig. 1 illustrates the application on a real sample microtome section of a painting in Bylapox resin. The sample is composed of three basic layers – the underlayer, under-painting and painting. Results of the analysis are presented in fig. 2 and 3.

P14

X-RAY POWDER DIFFRACTION IN FORENSIC PRACTICE

M. Kotrlý¹, P. Bezdička²

¹Institute of Criminalistics Prague, Strojnicka 27, PO box 62/KUP, 170 82 Prague 7, Czech Republic

²Institute of Inorganic Chemistry ASCR, 250 68 Rez, Czech Republic
kotrly_kup@email.cz

Introduction

The majority of analyses in forensic field deals with determination and comparisons of various evidence and materials. Often there is little or nothing known about them and in a crime lab one can meet very broad spectrum of various materials. Here lies the fundamental difference as compared with other analytical labs and institutes that are usually specialized more or less in certain material group. From this point of view the benefit of XRD methods is very significant, because they usually enable direct phase analysis (if the material to be examined is of crystal structure). Of course, not even XRD methods are omnipotent and are usually used in combination with other methods (mainly SEM-EDS/WDS, optical microscopy, XRF, FTIR etc.).

Recently there has been a trend in the forensic field to determine the phases by minimum of two independent methods. The conclusions of expert opinions are the basis for decisions made by bodies responsible for penal proceedings, i.e. deciding about guilt and punishment, and

therefore the results must be of the highest level of credibility. Here the role of XRD method is replaceable only with difficulty because it enables the performance of phase analysis on physically different principle than the majority of standard analytical methods for both inorganic and organic basis.

Methodology

In forensic science practice XRD methods can be used namely for analyses of mineral phases in soils, inorganic and organic phases in pigments and coating compositions, gemologic objects, inorganic and organic phases of post-blast residues, explosives components and pyrotechnic compositions, drug analysis (including semi-quantitative analysis) and other pharmaceutical and cosmetic products, building materials and their relics – abrasions, microparticles, metals and alloys (including abrasions), plastics and polymers, fillers and additives in papers and

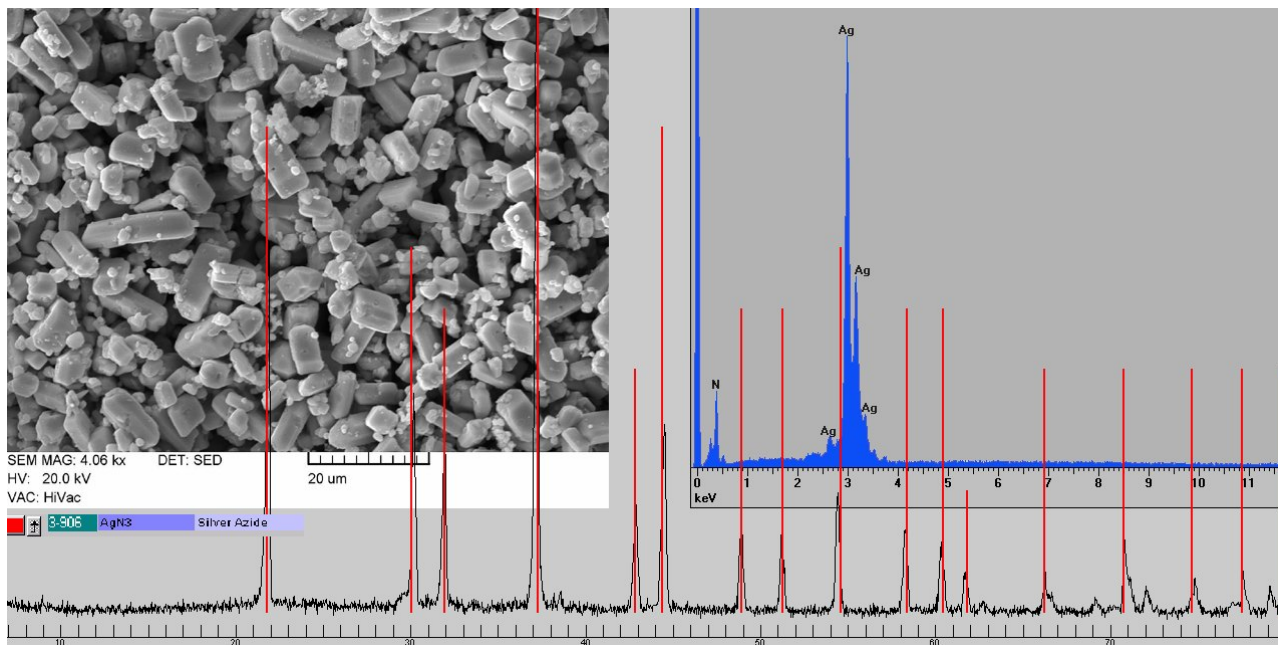


Fig. 1. The identification of silver azide presented as unknown material from domiciliary search (left SEM picture, right EDS spectra).

other products, and last but not least also in completely “unknown” samples (powders in extortion letters etc.).

Advantages of XRD methods in the forensic field lie in their complexity, in the possibility to analyze relatively small-volume samples, in their relative non-destructiveness, preservation of material after the analysis for prospective further examinations or revisions, and a relatively precise semi-quantitative phase analysis in a mixture.

Quite important are applications of XRD methods in the sphere of explosives and blaster agents analyses. Other methods can have problems with unambiguous phase analysis (e.g. azides or fulminates of heavy metals), possibly also with the specimen preparation for analysis of high explosive materials. Fig. 1 illustrates the identification of silver azide presented as unknown material from domiciliary search.

Recently, X-ray powder microdiffraction has started to gain ground. The term XRD microdiffraction appeared at the end of the 1990s. The microbeam in this case means

synchrotron radiation or radiation focused by polycapillary primary optics, which gives sufficient strength for diffraction data collection from a small area in reasonable time.

Test measurements for forensic application are made on an X’PertPRO diffractometer made by a Dutch company PANalytical. It is a combination of a common X-ray tube, a capillary, which focuses the X-ray beam into the diameter of 0.1 mm, and a position-sensitive detector. The application of microdiffraction in forensic field is of great importance because for the first time the size of the analyzed area is getting to the level comparable to other microscopic identification methods, and further it is possible to analyze common samples without any adjustment or change. Fig 2 shows the example of a bullet adjustment with abrasion relics of metals in the X’PertPRO diffractometer. The result of a conventional Bragg-Brentan method measurement (fig. 3 – lower curve), where the X-ray tube moves by the omega angle and the detector by theta angle on condition that $w = q$, showed that the most intensive diffraction line of aluminium (111) overlaps with b line from the most intensive

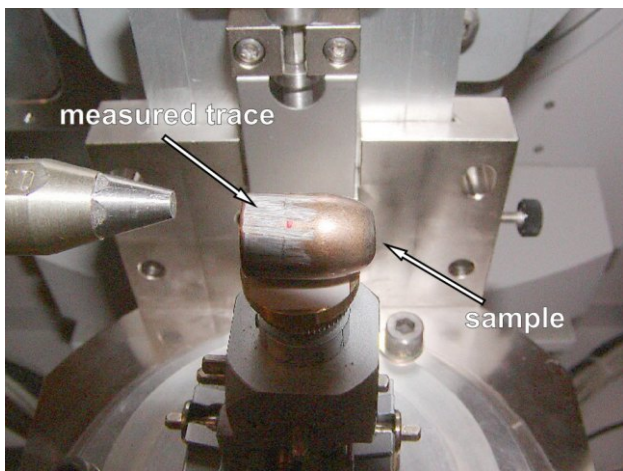


Fig. 2. Example of a bullet adjustment with abrasion relics of metals in the X’PertPRO diffractometer.

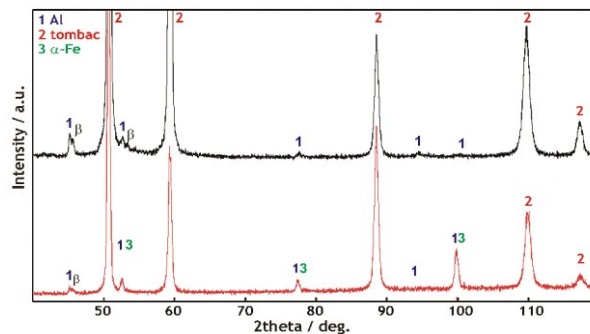


Fig. 3. Powder diffraction patterns of abrasions on the surfaces of 9 mm bullets Fe-tombac clad.



line of tombac (111). Furthermore, well noticeable are diffraction lines of ferritic steel from bullet core cladding. The diffraction line (211) of ferrite, which lies approx. next to 100 degrees 2theta, has significantly higher intensity than would be appropriate to the structure. This can be explained by the material stress of the rolled bullet jacket.

Another operating practice was chosen for the second measurement of the same spot to increase the contribution of surface layers to the whole analytical signal. In this case the incidence angle between the X-ray tube and the sample surface being measured was constant ($w = 7^\circ$) and only the detector was moving. This method of measurement results in a drop of penetration depth of X-radiation into the sample (with more significant contribution of surface layers of

the sample). With low (and constant) angle of incidence there is at the same time larger sample area radiated (fig. 3 – upper curve). Increase in Al contribution is noticeable and it is possible to distinguish clearly between aluminium line (111) and a tombac beta line (111). At the same time the diffraction lines of ferrite practically disappeared.

Acknowledgements

XRD methods at Institute of Criminalistics Prague were supported by grant-aided projects of the Czech Republic Ministry of Interior RN 19961997008, RN 19982000005, RN 20012003007 and RN 20052005001.

P15

STUDIES OF THE KINETICS OF THE CRYSTALLIZATION OF AMORPHOUS CHALCOGENIDE FILMS

E. Kotulanová¹, P. Bezdička¹, T. Grygar¹, T. Wagner², J. Gutwirt²

¹*Institute of Inorganic Chemistry AS CR, Rez, 250 68*

²*University of Pardubice, Department of General and Inorganic Chemistry, Legion's Sq. 565, 53210 Pardubice, Czech Republic, evulekotule@iic.cas.cz*

Amorphous chalcogenide films (amorphous chalcogenides of Ge, As, Sb, Te, Ag, In and other elements, with binary or multi-component compositions) have many potential and current applications in microoptics, photonic crystals and optical memories. Optically or electrically recorded memories are currently 'hot' scientific topic. The recording mechanism is an optically or electrically induced reversible phase transition between amorphous and crystalline states or reversible local change in the films composition.

Amorphous films of different composition $(\text{Ag}_x(\text{Sb}_{0.33}\text{S}_{0.67})_{100-x})$, where x was between 0 and 25 at.% Ag, resp.

$\text{Ag}_x(\text{As}_{0.33}\text{S}_{0.67})_{100-x}$, where x was between 0 and 35 at.% Ag), were prepared by pulsed laser deposition and optically induced silver dissolution into the binary chalcogenides deposited by vacuum evaporation techniques. Optically induced crystallization was demonstrated in films and the kinetics of the crystallization were studied by powder X-ray microdiffraction (micro-pXRD). A microdiffractometer with monocapillary primary optics and x , y , z -stage enables analysis from spot with a diameter of 0.15 mm.